Synthesis, Structure, and Catalytic Behavior of *rac*-1,1′-(3-Oxapentamethylene)-Bridged Bis(indenyl) *ansa*-Lanthanidocenes

Changtao Qian,* Gang Zou, Yaofeng Chen, and Jie Sun

Laboratory of Organometallic Chemistry, Shanghai Institute of Organic Chemistry, Chinese Academy of Science, 354 Fenglin Road, Shanghai 200032, China

Received December 11, 2000

A series of chiral 1,1′-(3-oxapentamethylene)-bridged bis(indenyl) *ansa*-lanthanidocenes have been high stereoselectively synthesized. The reaction of $YbCl_3$ with $O(CH_2CH_2C_9H_6K)_2$ in THF provided a *rac*/*meso* mixture of $[O(CH_2CH_2C_9H_6)_2]YbCl(THF)$; the major diastereomer formed is racemic. The *rac*-$[O(CH_2CH_2C_9H_6)_2]YbCl(THF)$ (**1**) was isolated after recrystallization of a *rac*/*meso* mixture of $[O(CH_2CH_2C_9H_6)_2]YbCl(THF)$ in THF. Direct amidation (or alkylation) of the *rac*/*meso* lanthanidocene chloride mixtures in toluene provided solely pure racemic *ansa*-lanthanidocene amides $[O(CH_2CH_2C_9H_6)_2]LnN(SiMe_3)_2$ (Ln = Y (**2**), Pr (**3**), Nd (**4**), Yb (**5**), Lu (**6**)) and pure racemic *ansa*-lanthanidocene hydrocarbyls $[O(CH_2CH_2C_9H_6)_2]$-$LnCH_2SiMe_3$ (Ln = Dy (**7**), Yb (**8**)). The structures of **1** and **5** were determined by X-ray diffraction. The amide and hydrocarbyl complexes are efficient single-component catalysts for methyl methacrylate polymerization. The effects of solvent and reaction temperature on the polymerization were studied. Very high molecular weight ($M_n > 10^6$) iso-rich poly(MMA) was obtained at lower temperature, while low molecular weight moderately syndiotactic poly(MMA) was obtained at higher temperature. The polymerization behavior is proposed to be associated with *rac*/*meso* interconversion of the active center.

Introduction

Racemic *ansa*-lanthanidocenes have demonstrated isospecific polymerization of α-olefin.[1] The racemic isomer, therefore, normally is the desired product of metalation of the ligand. Unfortunately, in most cases some amount of the achiral *meso* isomer is also formed, necessitating an often tedious separation process. Introducing bulky substituents onto the cyclopentadienyl rings is the predominant approch to achieve high *rac*/*meso* selectivity. Bercaw et al. found that the α-substituent plays the key role in stereospecific synthesis of racemic *ansa*-lanthanidocenes with silylene-bridged cyclopentadienyl rings $[Me_2Si(C_5H_2\text{-}2\text{-}X\text{-}4\text{-}CMe_3)_2$, X = $SiMe_3$, CMe_3, H].[1a,2] Recently, several bis(indenyl) *ansa*-lanthanidocenes have been reported. Anwander et al. synthesized $Me_2Si(C_9H_5\text{-}2\text{-}Me)_2YN(SiHMe)_2$ utilizing amine elimination reaction, and the pure racemic isomer has been separated after recrystallization of the *rac*/*meso* mixture (3:1) in hydrocarbon solvent.[3] Broene et al. prepared $[Me_2Si(C_9H_5\text{-}2\text{-}Me)_2LnCl][LiCl(Et_2O)_2]$ (Ln = Yb, Y), both complexes are the *rac*/*meso* mixtures, and the *rac*/*meso* ratio is low. The $Me_2Si(C_9H_5\text{-}2\text{-}Me)_2YbN(SiMe_3)_2$ was also prepared, but it is the *meso* isomer.[4] Very recently, Schumann et al. reported on a method to stereoselective synthesize C_2-symmetric *ansa*-lanthanidocenes by reductive coupling of acenaphthylene with activated ytterbium or samarium.[5]

Poly(methyl methacrylate) [poly(MMA)] is an important polymer in materials and surface-coating industries. Recently, lanthanidocenes have been found to efficiently catalyze the living highly stereospecific polymerization of MMA. Yasuda's and Marks's groups have studied the activity of the C_{2v}- and C_1-symmetric lanthanidocenes for MMA polymerization.[6,7] Recently, we have reported the synthesis of C_s-symmetric lanthanidocenes and their catalytic behavior to MMA polymerization.[8] But until now, there are no reports about MMA polymerization initiated by C_2-symmetric *rac*-lanthanidocene. On the basis of our previous work on ether-bridged bis(indenyl) *ansa*-lanthanide halide and hydrocarbyl complexes,[9,10] we further synthesized

* Corresponding author. E-mail: qianct@pub.sioc.ac.cn. Fax: 0086-21-64166128.

(1) (a) Coughlin, E. B.; Bercaw, J. E. *J. Am. Chem. Soc.* **1992**, *114*, 7606. (b) Mitchell, J. P.; Hajela, S.; Brookhart, S. K.; Hardcastle, K. I.; Henling, L. M.; Bercaw, J. E. *J. Am. Chem. Soc.* **1996**, *118*, 1045. (c) Yasuda, H.; Irara, E. *Bull. Chem. Soc. Jpn.* **1997**, *70*, 1745. (d) Irara, E.; Nodono, M.; Katsura, K.; Adachi, Y.; Yasuda, H.; Yamagashira, M.; Hashimoto, H.; Kanehisa N.; Kai, Y. *Organometallics* **1998**, *17*, 3945.

(2) (a) Bunel, E.; Burger, B. J.; Bercaw, J. E. *J. Am. Chem. Soc.* **1988**, *110*, 976. (b) Yoder, J. C.; Day, M. W.; Bercaw, J. E. *Organometallics* **1998**, *17*, 4946.

(3) Herrmann, W. A.; Eppinger, J.; Spiegler, M.; Runte, O.; Anwander, R. *Organometallics* **1997**, *16*, 1813.

(4) Gilbert, A. T.; Davis, B. L.; Emge, T. J.; Broene, R. D. *Organometallics* **1999**, *18*, 2125.

(5) Fedushkin, I. L.; Dechert, S.; Schumann, *Angew. Chem., Int. Ed.* **2001**, *40*, 561.

(6) (a) Yasuda, H.; Yamamoto, H.; Yokota, K.; Miyake S.; Nakamura, A. *J. Am. Chem. Soc.* **1992**, *114*, 4908. (b) Yasuda, H.; Yamamoto, H.; Yamashita, M.; Yokota, K.; Nakamura, A.; Miyake, S.; Kai, Y.; Kanehisa, N. *Macromolecules* **1993**, *26*, 7134. (c) Yasuda, H.; Ihara, E. *Macromol. Chem. Phys.* **1995**, *196*, 2417.

(7) Giardello, M. A.; Yamamoto, Y.; Brard, L.; Marks, T. J. *J. Am. Chem. Soc.* **1995**, *117*, 3276.

(8) Qian, C.; Nie, W.; Sun, J. *Organometallics* **2000**, *19*, 4134.

(9) Qian, C.; Zou, G.; Sun, J. *J. Chem. Soc., Dalton Trans.* **1998**, 1607.

(10) Qian, C.; Zou, G.; Sun, J. *J. Chem. Soc., Dalton Trans.* **1999**, 519.

10.1021/om001060g CCC: $20.00
Publication on Web 06/06/2001

Scheme 1

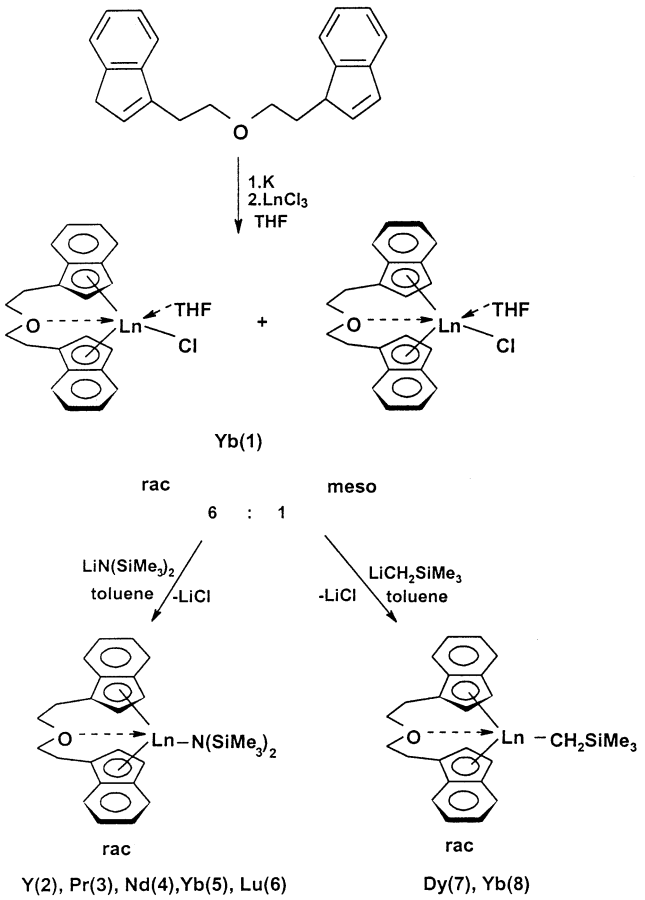

rac- and *meso*-[O($CH_2CH_2C_9H_6$)$_2$]YbCl(THF), *rac*-[O($CH_2CH_2C_9H_6$)$_2$]YbCl(THF) (**1**), *rac*-[O($CH_2CH_2C_9H_6$)$_2$]Ln$N(SiMe_3)_2$ (Ln = Y (**2**), Pr (**3**), Nd (**4**), Yb (**5**), Lu (**6**)), and *rac*-[O($CH_2CH_2C_9H_6$)$_2$] LnCH_2SiMe_3 (Ln = Dy (**7**), Yb (**8**)) and investigated the catalytic activity of amides and hydrocarbyls for MMA polymerization. Herein the results were reported in detail.

Results and Discussion

Synthesis. These chloride, hydrocarbyl, and amide complexes were synthesized as described in Scheme 1. A *rac*/*meso* mixture of [O($CH_2CH_2C_9H_6$)$_2$]YbCl(THF) was prepared by the reaction of $YbCl_3$ with O($CH_2CH_2C_9H_6K$)$_2$ in THF. Our previous results showed these kinds of complexes predominate racemic diastereomer.[9] The racemic isomer **1** was isolated by recrystallization of a *rac*/*meso* mixture of [O($CH_2CH_2C_9H_6$)$_2$]YbCl(THF) in THF. The reaction between [O($CH_2CH_2C_9H_6$)$_2$]LnCl(THF) (Ln = Y, Pr, Nd, Yb, Lu) and 1 equiv of Li$N(SiMe_3)_2$ in toluene at room temperature afforded solely *rac*-[O($CH_2CH_2C_9H_6$)$_2$]Ln$N(SiMe_3)_2$ (Ln = Y (**2**), Pr (**3**), Nd (**4**), Yb (**5**), Lu (**6**)) isomers in moderate yield. The solely racemic hydrocarbyl isomers **7** and **8** were synthesized in the procedure similar to that for *rac*-[O($CH_2CH_2C_9H_6$)$_2$]YCH_2SiMe_3,[10] by alkylation of [O($CH_2CH_2C_9H_6$)$_2$]LnCl(THF) (Ln = Dy, Yb) with LiCH_2SiMe_3 in toluene. It is worthy to note that pure racemic amides and hydrocarbyls can be obtained directly from the *rac*/*meso* lanthanidocene chloride mixtures. Thus tedious and complicated separation of isomer was avoided. All complexes are air- and moisture-sensitive. **1** is soluble in THF at room temperature and just slightly soluble in toluene, while the amide and hydrocarbyl complexes (**2**−**8**) are very soluble in THF, DME, toluene, and benzene and sparing soluble in hexane. Elemental analysis and spectroscopic data indicated the amide and hydrocarbyl complexes are solvent-free.

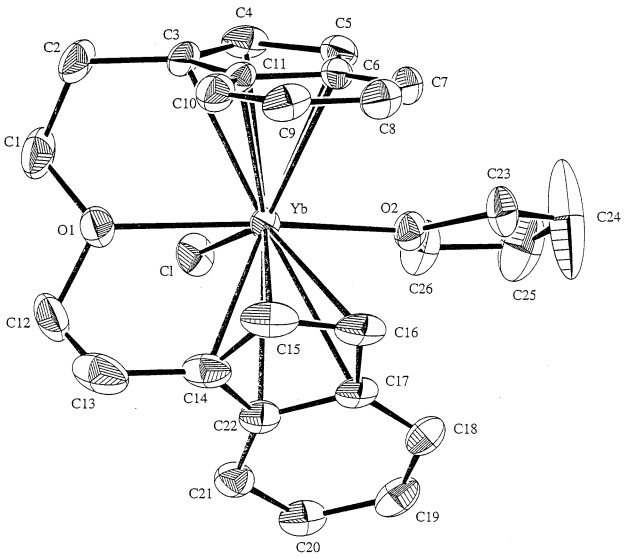

Figure 1. ORTEP diagram of *rac*-[O($CH_2CH_2C_9H_6$)$_2$]YbCl(THF) (**1**).

Spectroscopic Properties. The variable-temperature ^{1}H NMR spectra of diamagnetic amide **6** was recorded in [$^2H_8$]toluene and [$^2H_8$]tetrahydrofuran at −50, −25, 0, 30, and 50 °C. Similar to [O($CH_2CH_2C_9H_6$)$_2$]YCH_2SiMe_3 and [O($CH_2CH_2C_9H_6$)$_2$]LuCH_2SiMe_3,[10] only one set of resonances of protons of the complex were observed, indicating the presence of solely *rac* isomers in solution and no isomerization occurs in the range of the above-mentioned temperatures. The ^{1}H NMR spectrum of **2** is similar to that of **6**, implying that their structures should be essentially identical. Two five-membered ring protons of the bridged indenyl display different resonances, revealing **2** and **6** adopt the unsymmetric structure observed in their racemic chlorides and hydrocarbyls.[9,10] Protons of the $-SiMe_3$ group show two sets of signals at normal chemical shifts δ 0.05 and −0.25 ppm. Two $-SiMe_3$ groups are inequivalent in the ^{1}H NMR spectra, indicating hindered rotation of the amide group. ^{1}H NMR assignment was based on the chemical shifts and two-dimensional COSY and NOESY spectra of complex **2**. The presence of cross-peaks between H^1 and aromatic protons $H^{4'}$ and $H^{5'}$ and the absence of cross-peaks between $H^{1'}$ and aromatic protons confirm the unsymmetric structure of the *rac ansa*-lanthanidocene amide.

Molecular Structures. The structures of **1** and **5** were determined by single-crystal X-ray diffraction. ORTEP drawings are shown in Figures 1 and 2. The crystallographic data and refinements are given in Table 1, and selected structural data are listed in Table 2.

X-ray analysis reveals both complexes are racemic isomers in the solid state and crystallize in the monoclinic system. Space groups of **1** and **5** are $P2_1/n$ and $P2_1/a$, respectively. The intramolecular coordination of bridged oxygen was observed in both complexes. The distance between the bridge oxygen and the metal ion

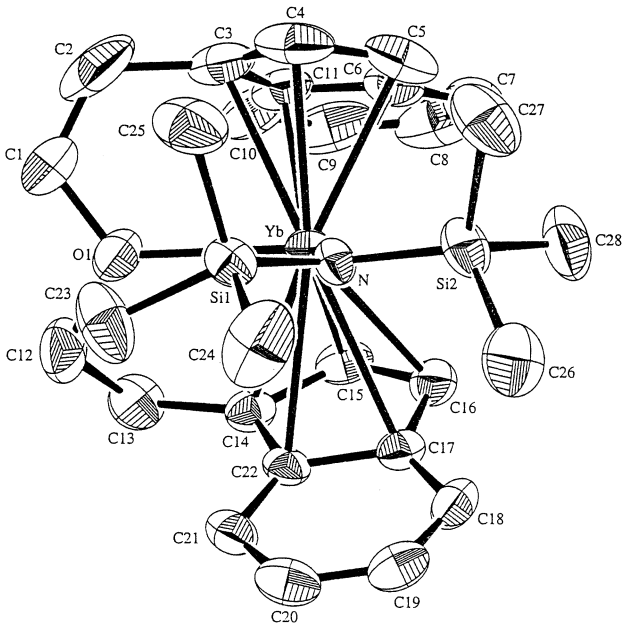

Figure 2. ORTEP diagram of *rac*-[O(CH$_2$CH$_2$C$_9$H$_6$)$_2$]YbN(SiMe$_3$)$_2$ (**5**).

Table 1. Details of the Crystallographic Data and Refinements

	1	**5**
formula	$C_{26}H_{28}O_2ClYb$	$C_{28}H_{38}ONSi_2Yb$
fw	581.00	633.83
cryst size, mm	0.20 × 0.30 × 0.40	0.20 × 0.20 × 0.30
color	dark green	dark green
cryst syst	monoclinic	monoclinic
space group	$P2_1/n$	$P2_1/a$ (#14)
a, Å	10.975(2)	14.245(5)
b, Å	10.094(1)	13.592(3)
c, Å	20.516(5)	14.287(4)
β, deg	97.97(2)	100.55(2)
V, Å^3	2250.7(7)	2719(1)
Z	4	4
D_{calcd}, Mg/m^3	1.714	1.548
F(000)	1148.00	1276.00
μ, cm^{-1}	42.93	35.47
$2\theta_{max}$ (deg)	45.0	51.0
no. of reflns collected	3149	5526
no. of ind reflns	2961	5508
no. of obsd data	2497	3360
no. of params	272	272
goodness of fit	1.58	1.36
final R, R_w[a]	0.023, 0.032	0.026, 0.034
$\Delta\rho_{max,min}$/e Å^{-3}	0.57, −0.87	1.30, −0.58

[a] $R = \Sigma||F_o| - |F_c||/\Sigma|F_o|$, $R_w = [\Sigma w(|F_o| - |F_c|)^2/\Sigma|F_o|^2]^{0.5}$.

in **1** is 2.422(4) Å, which agrees well with those in [O(CH$_2$CH$_2$C$_9$H$_6$)$_2$]LnCl(thf) (Ln = Nd, 2.507(4) Å; Ln = Gd, 2.470(5) Å; and Ln = Ho, 2.448(4) Å) after ionic radius corrections.[9] The Yb−O distance in **5** (2.395(3) Å) is shorter than that in **1** (2.422(4) Å), reflecting the comparatively low coordination number of Yb in **5**. One tetrahydrofuran molecule is coordinated to the central metal in **1**. The coordination geometry of the complex can be described as distorted trigonal bipyramidal with O(1) and O(2) apical if the indenyl ring is regarded as occupying a single polyhedral vertex. **5** is solvent-free and adopts distorted tetrahedral geometry. The X-ray data for **1** show highly unsymmetric metal−indenyl distances. One indenyl ligand shows η^5-coordination to a metal ion at a normal distance ranging from 2.634(5) to 2.700(5) Å, while the other is bonded to the Yb atom in η^3-mode (Yb−C (ring), 2.574(5), 2.634(5), 2.652(6) Å and 2.779(5), 2.794(5) Å). In **5**, Yb−indenyl distances of two indenyl ligands range from 2.593(4) to 2.769(5) Å and 2.568(6) to 2.735(5) Å, respectively. The bonding mode of the metal atom with indenyl ligands might be described as being partially slipped toward η^3- from η^5-mode. Usually, "Cp′$_2$LnN(SiMe$_3$)$_2$" derivatives display $^{\beta}$Si−Me−metal and ($^{\gamma}$C)H−metal agostic interactions.[8,11−14] However, in **5**, The long Yb−Si (3.352(2), 3.462(2) Å) and Yb−C (Yb−C(23) = 3.730(7), Yb−C(28) = 3.472(7) Å) distances indicate the absence of $^{\beta}$Si−Me−metal and ($^{\gamma}$C)H−metal agostic interactions. As a result,

Table 2. Selected Bond Lengths (Å) and Angles (deg) for Complexes 1 and 5

	1	**5**
	Bond Lengths	
Yb−Cl	2.542(1)	2.199(4)
Yb−N	2.422(4)	2.395(3)
Yb−O(1)		
Yb−O(2)	2.407(4)	
Yb−C(3)	2.658(5)	2.628(5)
Yb−C(4)	2.634(5)	2.568(6)
Yb−C(5)	2.645(5)	2.613(6)
Yb−C(6)	2.692(5)	2.733(5)
Yb−C(11)	2.700(5)	2.735(5)
Yb−C(14)	2.652(6)	2.649(5)
Yb−C(15)	2.574(5)	2.593(4)
Yb−C(16)	2.634(5)	2.627(5)
Yb−C(17)	2.794(5)	2.769(5)
Yb−C(22)	2.779(5)	2.752(4)
C(1)−C(2)	1.498(9)	1.35(1)
C(12)−C(13)	1.49(1)	1.512(8)
N−Si(1)		1.726(4)
N−Si(2)		1.722(4)
	Bond Angles	
Cl−Yb−O(1)	78.9(1)	
Cl−Yb−O(2)	81.94(9)	
O(1)−Yb−O(2)	160.9(1)	
O(1)−Yb−N		110.4(1)
Yb−N−Si(1)		123.3(2)
Yb−N−Si(2)		117.0(2)
Si(1)−N−Si(2)		118.7(2)
N−Si(1)−C(23)		111.3(2)
N−Si(1)−C(24)		114.0(2)
N−Si(1)−C(25)		114.3(3)
N−Si(2)−C(26)		
N−Si(2)−C(27)		
N−Si(2)−C(28)		
O(1)−C(1)−C(2)		
O(1)−C(12)−C(13)		
		114.7(3)
		112.0(3)
		113.0(2)
	107.7(5)	117.6(7)
	106.1(6)	108.9(5)
C(1)−C(2)−C(3)	112.5(5)	117.3(6)
C(12)−C(13)−C(14)	112.0(5)	111.2(4)
Yb−O(1)−C(1)		124.5(4)
	Dihedral Angles	
	51.12	49.73

(11) (a) den Haan, K. H.; de Boer, J. L.; Teuben, J. H.; Spek, A. L.; Kojic-prodic, B.; Hays, G. R.; Huis, R. *Organometallics* **1986**, *5*, 1726. (b) Schumann, H.; Rosenthal, E. C. E.; Kociok-köhn, G.; Molander, G. A.; Winterfeld, J. *J. Organomet. Chem.* **1995**, *496*, 233.

(12) Lee, M. H.; Hwang, J.-E.; Kim, Y.; Kim, J.; Do, Y. *Oranometallics* **1999**, *18*, 5124.

(13) (a) Tilley, T. D.; Andersen, R. A.; Zalkin, A. *Inorg. Chem.* **1984**, *23*, 2271. (b) Evans, W. J.; Anwander, R.; Ziller, J. W.; Khan, S. I. *Inorg. Chem.* **1995,** *34*, 5927.

(14) Giardello, M. A.; Conticello, V. P.; Brard, L.; Sabat, M.; Rheingold, A. L.; Stern, C. L.; Marks, T. J. *J. Am. Chem. Soc.* **1994**, *116*, 10212.

the complex exhibits small difference in the ∠Ln−C−Si angle (6.3°), similar to that observed in (S)−Me_2Si-(C_5Me_4)−(+)-neomenthyl(C_5H_3)SmN($SiMe_3$)$_2$,[14] which also does not exhibit $^{\beta}$Si−Me−metal and ($^{\gamma}$C)H−metal agostic interactions. Furthermore, the angles between N−Si−C fall in a very small range (112.0(3)−114.7(3) Å). The distance between the Yb atom and the N atom is 2.199(4) Å. In contrast to the silylene-bridged bis(indenyl) lanthanidocene amide $Me_2Si(C_9H_5Me\text{-}2)_2YN(SiHMe_2)_2$[3] and the dimethylene-bridged bis(indenyl) lanthanidocene amide $C_2H_4(C_9H_6)_2YN(SiMe_3)_2$,[4] the O(1)−Yb−N angle in **5** is 110.4(1)°, indicating the orientation of the amide group parallels the indenyl planes, *syn* to the six-membered proton of one of the bridged indenyl rings and *anti* to that of the other indenyl ring. A similar arrangement has also been found in the alkyl complex [O($CH_2CH_2C_9H_6$)$_2$]$YCH_2(SiMe_3)$.[10] This interesting arrangement is perhaps adopted to avoid the repulsion between the amide (or alkyl) group and the edges of the indenyl planes since the "wide porton" of the *ansa*-metallocene is significantly narrowed by the rigid five-atom bridge. It is evident that efficient minimization of the nonbonded repulsion could be achieved in the racemic isomer, since the amide (or alkyl) group could not only avoid simultaneous interactions with the six-membered portons of the two bridged indenyl rings but also further minimize the nonboned repulsion by orienting away from the *syn* indenyl plane. However, a strong repulsion could be anticipated in the *meso* isomer whether the alkyl group orients toward the narrow or wide porton of the *ansa*-metallocene wedge. The *ansa*-lanthanidocene chlorides existed as a equilibrium of the *rac*/*meso* mixture in THF.[9,10] Highly stereoselective formatiom of pure racemic amide and hydrocarbyl complexes from the *rac*/*meso* mixture of chlorides may occur via the epimerization of *meso* chlorides to racemic chlorides during the amidation/alkylation. Similar epimerizaton was observed by Marks et al. for some C_1-symmetric lanthanidocene chlorides during the amidation/alkylation.[14,15] It is interesting that *rac*/*meso* stereoselectivity could be dictated by the nonboned interactions between the indenyl planes and the amide (or amide) group instead of the two bridged indenyl rings. A significant difference between C(1)−C(2) (1.35(1) Å) and C(12)−C(13) (1.512(8) Å) is observed, which has not been observed in the chloride and hydrocarbyl complex bearing the same indenyl ligand.[9,10] It is concluded that minimization of nonbonded repulsion between the indenyl ring and the amide group in the more crowed amides occurred not only by adopting a racemic isomer but also through the distortion of the ether bridge.

Polymerization of Methyl Methacrylate. The amide and hydrocarbyl complexes were applied for initiating methyl methacrylate polymerization. The effects of solvent on the polymerization initiated by *rac*-[O($CH_2CH_2C_9H_6$)$_2$]$YN(SiMe_3)_2$ (**2**) and *rac*-[O(CH_2CH_2-C_9H_6)$_2$]YCH_2SiMe_3 (**9**)[10] were studied (Table 3). It was found that **2** and **9** show higher activity in THF and DME than in toluene. The solvent also affects the polymer tacticity. THF and DME favor syndiospecific polymerization, but toluene favors isospecific polymerization.

Table 3. Effects of Solvent on the MMA Polymerization[a]

catalyst	solvent	conv (%)	rr	mr	mm
2	toluene	5	19	19	62
	DME	30	27	21	52
	THF	26	27	21	52
9	toluene	14	45	25	30
	DME	42	56	28	16
	THF	31	56	29	15

[a] Conditions: cat./MMA (mol/mol) = 1:500, polymerization time = 3 h, T = 0 °C, MMA/solvent (v/v) = 1.

The reaction temperature has great effects on the MMA polymerization (Table 4). The activities of **2** and **9** are very low at 30 °C. Their activities increase by lowering the reaction temperature. **2** and **9** show the highest activity around −25 and −50 °C, respectively. Lowering the reaction temperature to −50 °C for **2** and −78 °C for **9** resulted in no polymerization. **2** and **9** initiate moderately syndiospecific polymerization of MMA at higher temperature, such as at 30 to 5 °C for **2** and at 30 to −35 °C for **9**. The mm content increased with reaction temperature decreasing. **2** produced poly(MMA) of 63% isotacticity at −25 °C, and **9** produced poly(MMA) of 66% isotacticity at −50 °C. At higher reaction temperature, the molecular weight of poly(MMA) is low and the molecular weight distribution is narrow. The molecular weight increases dramatically when the reaction temperature was lowered, but the molecular weight distribution becomes broad. Upon further lowering of the reaction temperature, the molecular weight distribution becomes narrow. A very high molecular weight (M_w = 1.88 × 10^6) with narrow molecular weight distribution (M_w/M_n = 1.67) polymer is produced with **9** at −50 °C. The polymerization behavior was proposed to be associated with *rac*/*meso* interconversion of the active center. *ansa*-Metallocenes usually exist in two possible isomers: a *rac* isomer and a *meso* isomer. Some *ansa*-metallocenes undergo *rac*/*meso* interconversion at suitable condition. It is commonly promoted by the coordinating solvent THF, ether, and Li^+ salt.[2b,16] Such interconversion was also observed in the ether-bridged indenyl lanthanidocene chlorides in THF.[9,10] According to the coordinating polymerization mechanism proposed by Yasuda, the active center in MMA polymerization is the enolate complex [O(CH_2-$CH_2C_9H_6$)$_2$]$LnOC(OCH_3)$═$C(CH_3)X$.[5] At lower temperature, the enolate complex remains the racemic isomer, which initiates MMA isospecific polymerization. Moderately syndiospecific polymerization at higher temperature can be attributed to the *rac*/*meso* interconversion of the enolate complex. MMA can act as the coordinating molecule, and the *meso* isomer is responsible for syndiospecific polymerization of MMA. Our more recent results indicate *meso*-[O($CH_2CH_2C_9H_6$)$_2$]Sm(II) initiates moderately syndiospecific polymerization of MMA at 5 and −78 °C. The *rac*/*meso* interconversion of the enolate

(15) Harr, C. M.; Stern, C. L., Marks T. J. *Organometallics* **1996**, *15*, 1765.

(16) (a) Hultzsch, K. C.; Spaniol, T. P.; Okuda, J. *Organometallics* **1997**, *16*, 4845. (b) Diamond, G. M.; Rodewald, S.; Jodan, R. F. *Organometallics* **1995**, *14*, 5. (c) Diamond, G. M.; Jodan, R. F.; Petersen, J. L. *Organometallics* **1996**, *15*, 4030. (d) Christopher, J. N.; Diamond, G. M.; Jodan, R. F.; Petersen, J. L. *Organometallics* **1996**, *15*, 4038. (e) Diamond, G. M.; Jodan, R. F.; Petersen, J. L. *Organometallics* **1996**, *15*, 4045.

Table 4. Polymerization of MMA at Different Temperatures[a]

catalyst	solvent	T (°C)	conv (%)	rr	mr	mm	$M_w \times 10^{-3}$	$M_n \times 10^{-3}$	M_w/M_n	T_g (°C)
2	THF	30	6	45	32	23	38.8	15.2	2.55	
		5	13	43	28	29				
		0	26	27	21	52	263.2	70.6	3.73	
		−25	62	18	19	63	846	480	1.76	
		−50					inactive			
9	DME	30	22	53	30	17	25.4	15.3	1.66	110
		0	42	56	28	16	77.7	30.1	2.58	113
		−25	31	54	26	20	424	96.9	4.37	106
		−50	56	18	16	66	1883	1126	1.67	66
		−78					inactive			
	toluene	−25	28	30	20	50				

[a] Conditions are the same as those of Table 3.

Table 5. Polymerization of MMA with Different Rare Earth Metallocenes[a]

catalyst	solvent	T (°C)	conv (%)	rr	mr	mm
rac-[O($CH_2CH_2C_9H_6$)$_2$]NdN($SiMe_3$)$_2$ (**4**)			30	44	28	28
rac-[O($CH_2CH_2C_9H_6$)$_2$]YN($SiMe_3$)$_2$ (**2**)			13	43	28	29
rac-[O($CH_2CH_2C_9H_6$)$_2$]YbN($SiMe_3$)$_2$ (**5**)[b]	THF	5	11	54	32	14
rac-[O($CH_2CH_2C_9H_6$)$_2$]LuN($SiMe_3$)$_2$ (**6**)[b]			13	57	31	12
rac-[O($CH_2CH_2C_9H_6$)$_2$]DyCH_2SiMe_3 (**7**)			77	50	28	22
rac-[O($CH_2CH_2C_9H_6$)$_2$]YCH_2SiMe_3 (**9**)	DME	0	42	56	28	16
rac-[O($CH_2CH_2C_9H_6$)$_2$]YbCH_2SiMe_3 (**8**)			37	52	27	21

[a] Conditions are the same as those of Table 3. [b] Polymerization time = 9 h.

complex at the prevailing polymerization is demonstrated by a ^{1}H NMR experiment: addition 0.5 equiv of ^{i}PrOH, representing the approximate steric bulk of MMA, to a solution of **9** in [$^2H_8$]tetrahydrofuran in an NMR tube at room temperature. Besides *rac*-[O($CH_2CH_2C_9H_6$)$_2$]YCH_2SiMe_3 and *rac*-[O($CH_2CH_2C_9H_6$)$_2$]YO^iPr, the *meso*-[O($CH_2CH_2C_9H_6$)$_2$]YO^iPr was observed. The ratio of *meso*-[O($CH_2CH_2C_9H_6$)$_2$]YO^iPr to *rac*-[O($CH_2CH_2C_9H_6$)$_2$]YO^iPr is about 1:3.

Polymerization of MMA with different metal ions of amides and hydrocarbyls was also investigated (Table 5). The activities of the amides decrease in the following order: **4** (Nd) > **2** (Y) > **5** (Yb) ≈ **6** (Lu), and the decreasing order **7** (Dy) > **9** (Y) > **8** (Yb) is observed in the case of hydrocarbyls. Those orders are in good agreement with the decreasing order of ionic radii, Nd (0.995 Å) > Dy (0.908 Å) > Y (0.88 Å) > Yb (0.858 Å) ≈ Lu (0.848 Å), similar to that found in (C_5Me_5)$_2$LnMe(THF)$_2$.[5b]

Conclusion

In summary, a series of chiral 1,1′-(3-oxapentamethylene)-bridged bis(indenyl) *ansa*-lanthanidocenes were highly stereoselectively synthesized. The *rac*-[O($CH_2CH_2C_9H_6$)$_2$]YbCl(THF) (**1**) was isolated after recrysallization of a *rac*/*meso* mixture of [O($CH_2CH_2C_9H_6$)$_2$]YbCl(THF) in THF, and its structure was characterized by X-ray diffraction. Pure racemic *ansa*-lanthanidocene amides *rac*-[O($CH_2CH_2C_9H_6$)$_2$]LnN($SiMe_3$)$_2$ (Ln = Y (**2**), Pr (**3**), Nd (**4**), Yb (**5**), Lu (**6**)) and hydrocarbyls *rac*-[O($CH_2CH_2C_9H_6$)$_2$]LnCH_2SiMe_3 (Ln = Dy (**7**), Yb (**8**)) were conveniently synthesized by direct amidation (or alkylation) of the *rac*/*meso* mixture of lanthanidocene chlorides in toluene. *Rac*/*meso* stereoselectivity is dictated by the nonboned interactions between the indenyl planes and the amide (or hydrocarbyl) group. The amide and hydrocarbyl complexes are active for the polymerization of methyl methacrylate. The tacticity of the polymer was greatly affected by the polymerization temperature. The polymerization behavior is proposed to be associated with *rac*/*meso* interconversion of the active center.

Experimental Section

All operations involving organometallics were carried out under an inert atmosphere of argon using standard Schlenk techniques. Tetrahydrofuran, toluene, and 1,2-dimethoxyethane were distilled under argon from sodium−benzophenone prior to use. Anhydrous lanthanide chlorides were prepared according to the literature. The dipotassium salt of 1,1′-(3-oxapentamethylene)-bridged bis(indenyl) [($K_2C_9H_6CH_2CH_2$)O] and *rac*-[O($CH_2CH_2C_9H_6$)$_2$]YCH_2SiMe_3 (**9**) were synthesized following the procedures previously reported.[9,10] *n*-Butyllithium was obtained from Aldrich. The [$^2H_8$]tetrahydrofuran and [$^2H_8$]toluene were degassed and dried over Na/K alloy. Methyl methacrylate was distilled over CaH_2 and stored over 3 Å molecular sieves under argon. IR and FT-Raman spectra were recorded using Perkin-Elmer 983 and Bio-Rad FT-Raman spectrometers. Mass spectra was carried out with a HP5989A spectrometer (50−400 °C, 1.3 kV). ^{1}H NMR was performed on a Bruker Am-300 (300 HMz) spectrometer, and the variable-temperature ^{1}H NMR spectra of diamagnetic amide **6** were recorded on an Inova-600 (600 HMz) spectrometer. Elemental analyses were performed by the Analytical Laboratory of Shanghai Institute of Organic Chemistry. Gel permeation chromatographic analyses were performed by the Institute of Physical and Chemical research (RIKEN), Hirosawa 2-1, Japan. The *o*-dichlorobenzene was used as the eluent, and the system was calibrated using polystyrene standards. Glass transition points of poly(MMA) were measured with Perkin-Elmer Pyris-1 at a rate of 10 °C/min.

Synthesis of a *Rac*/*Meso* Mixture of O($CH_2CH_2C_9H_6$)$_2$]-YbCl(THF) and *rac*-[O($CH_2CH_2C_9H_6$)$_2$]YbCl(THF) (1). To a suspension of $YbCl_3$ (0.78 g, 2.78 mmol in 50 mL of THF) at −78 °C was added by syringe a THF solution of [($K_2C_9H_6CH_2CH_2$)O] (2.78 mmol in 30 mL[3]).The mixture was stirred for 2 days. The precipitate was separated, and the clear solution was concentrated until a solid appeared. The product was washed with cool THF (10 mL) and dried in vacuo at room temperature, affording 0.67 g (41%) of a *rac*/*meso* mixture of [O($CH_2CH_2C_9H_6$)$_2$]YbCl(THF). Anal. Calcd for $C_{26}H_{28}O_2ClYb$:

C, 53.75; H, 4.82. Found: C, 53.97; H, 5.10. EI mass spectrum (70 eV, 50−400 °C based on ^{174}Yb): *m*/*z* 509 (75.66, [M − thf]$^+$), 474 (31.25, [M − THF − Cl]$^+$), and 141 (100%). IR (cm^{-1}): 3060(m), 3036(m), 3030(sh), 2930(sh), 2900(m), 2880(sh), 1684(w), 1609(w), 1459(w), 1438(w), 1399(w), 1338(m), 1259(m), 1233(m), 1205(m), 1120(s), 1082(m), 1056(m), 1024(m), 990(m), 965(m), 918(m), 871(m), 803(m), 772(s), 743(m), 722(s), 673(m), 439(m), 230(w). *rac*-[O(CH$_2$CH$_2$C$_9$H$_6$)$_2$]YbCl(THF) (**1**) was isolated by recrystallization of *rac*/*meso* mixture of [O(CH$_2$-CH$_2$C$_9$H$_6$)$_2$]YbCl(THF) in THF.

Synthesis of *rac*-[O(CH$_2$CH$_2$C$_9$H$_6$)$_2$]YN(SiMe$_3$)$_2$ (2). To a suspension of 2.95 g (5.94 mmol) of [O(CH$_2$CH$_2$C$_9$H$_6$)$_2$]YCl-(THF) in 60 mL of toluene was added 1.0 g (5.94 mmol) of LiN-(SiMe$_3$)$_2$ at room temperature. The resulting suspension was stirred for 2 days under argon. The precipitate was separated by centrifugation, and the clear solution was concentrated until a solid appeared. The precipitate was separated again, and the clear solution was cooled to −30 °C. A total of 2.42 g (74%) of **2** was obtained as colorless crystals. Anal. Calcd for C$_{28}$H$_{38}$-ONSi$_2$Y: C, 61.20; H, 6.92; N, 2.55. Found: C, 61.11; H, 6.96; N, 2.80. ^{1}H NMR (300 HMz, [^{2}H$_8$]THF, 25 °C): δ 7.7 (m, 1H, H$^{6'}$, aromatic), 7.65 (m, 1H, H$^{3'}$, aromatic), 7.25 (m, 2H, H^3, H,^{6} aromatic), 7.10 (m, 2H, H$^{4'}$, H$^{5'}$, aromatic), 6.85 (m, 2H, H,^{4} H,^{5} aromatic), 6.40 (d, J = 3.1 Hz, 1H, H$^{1'}$), 5.95 (dd, J_1 = 3.1 Hz, J_2 = 0.6 Hz, 1H, H$^{2'}$), 4.95 (d, J = 3.2 Hz, 1H, H$^{2'}$), 4.75 (dt, J_1 = 14.8, J_2 = 5.3, 1H, OCH$^{n'}$H$^{m'}$), 4.65 (d, J = 3.0 Hz, 1H, H^1), 4.60 (dt, J_1 = 15.1, J_2 = 4.3, 1H, OCH^{n}H^m, overlapped with H^1), 4.20 (m, 2H, OCH$^{n'}$H$^{m'}$, OCH^{n}H^m), 3.25 (dt, J_1 = 14.8, J_2 = 5.0, 1H, CH$^{b'}$H$^{a'}$), 2.95 (m, 1H, CH$^{b'}$H$^{a'}$), 2.85 (J_1 = 14.8, J_2 = 5.3, 1H, CH^{b}H^a, overlapped with H^a), 2.80 (m, 1H, CH^{a}H^b), 0.05 (s, 9H, NSi(CH$_3$)$_3$), −0.30 (s, 9H, NSi(CH$_3$)$_3$). FT-Raman (cm^{-1}): 3088(m), 3047(m), 2980(m), 2940(m), 2895(s), 1606(w), 1531(m), 1484(m), 1469(sh), 1445(m), 1394(w), 1337(s), 1284(w), 1233(w), 1188(m), 1132(w), 1010(m), 873(m), 741(m), 693(m), 669(m), 618(m), 532(w), 444(w), 393(w), 290(m), 232(m), 150(s), 121(m).

Synthesis of *rac*-[O(CH$_2$CH$_2$C$_9$H$_6$)$_2$]PrN(SiMe$_3$)$_2$ (3). A procedure similar to that for complex **2** was adopted for [O(CH$_2$CH$_2$C$_9$H$_6$)$_2$]PrCl(THF) (1.36 g, 2.48 mmol) and LiN-(SiMe$_3$)$_2$ (0.42 g, 2.51 mmol), which afforded **3** as yellow-green crystals (0.91 g, 61%). Anal. Calcd for C$_{28}$H$_{38}$ONSi$_2$Pr: C, 55.91; H, 6.32; N, 2.33. Found: C, 55.82; H, 6.25; N, 2.54. FT-Raman (cm^{-1}): 3086(w), 3044(m), 2953(w), 2890(w), 1603(w), 1529(m), 1483(m), 1468(sh), 1443(m), 1392(sh), 1334(s), 1285(m), 1232(w), 1186(m), 1130(w), 1075(w), 1009(m), 872(m), 740(m), 672(m), 628(w), 606(m), 529(w), 444(w), 386(w), 281(m), 228(m), 144(s), 121(m).

Synthesis of *rac*-[O(CH$_2$CH$_2$C$_9$H$_6$)$_2$]NdN(SiMe$_3$)$_2$ (4). A procedure similar to that for complex **2** was adopted for [O(CH$_2$CH$_2$C$_9$H$_6$)$_2$]NdCl(THF) (2.68 g, 4.86 mmol) and LiN-(SiMe$_3$)$_2$ (0.82 g, 4.91 mmol), which afforded **4** as green crystals (2.07 g, 70%). Anal. Calcd for C$_{28}$H$_{38}$ONSi$_2$Nd: C, 55.63; H, 6.29; N, 2.32. Found: C, 55.62; H, 6.39; N, 2.42. FT-Raman (cm^{-1}): 3086(m), 3044(m), 2947(m), 2895(s), 1603(w), 1529(m), 1483(m), 1468(sh), 1443(m), 1392(sh), 1334(s), 1284(m), 1231(w), 1186(m), 1127(w), 1075(w), 1009(m), 872(w), 740(m), 672(w), 628(m), 606(m), 529(w), 445(w), 386(w), 282(m), 229(m), 144(s), 121(m).

Synthesis of *rac*-[O(CH$_2$CH$_2$ C$_9$H$_6$)$_2$]YbN(SiMe$_3$)$_2$ (5). A procedure similar to that for complex **2** was adopted for [O(CH$_2$CH$_2$C$_9$H$_6$)$_2$]YbCl(THF) (1.37 g, 2.36 mmol) and LiN-(SiMe$_3$)$_2$ (0.40 g, 2.40 mmol), which afforded **5** as dark green crystals (0.85 g, 57%). Anal. Calcd for C$_{28}$H$_{38}$ONSi$_2$Yb: C, 53.08; H, 6.00; N, 2.21. Found: C, 52.51; H, 6.13; N, 2.13. FT-Raman (cm^{-1}): 3080(m), 3040(m), 3043(m), 2898(s), 1528(m), 1480(m), 1470(sh), 1444(m), 1336(s), 1191(m), 1161(w), 1003(m), 742(m), 620(m).

Synthesis of *rac*-[O(CH$_2$CH$_2$ C$_9$H$_6$)$_2$]LuN(SiMe$_3$)$_2$ (6). A procedure similar to that for complex **2** was adopted for [O(CH$_2$CH$_2$C$_9$H$_6$)$_2$]LuCl(THF) (3.06 g, 5.25 mmol) and LiN-(SiMe$_3$)$_2$ (0.88 g, 5.27 mmol), which afforded **6** as colorless crystals (2.19 g, 66%). Anal. Calcd for C$_{28}$H$_{38}$ONSi$_2$Lu: C, 52.91; H, 5.98; N, 2.20. Found: C, 53.43; H, 6.19; N, 2.34. ^{1}H NMR (300 HMz, [^{2}H$_8$]THF, 25 °C): δ 7.65 (m, 2H, H$^{3'}$, H$^{6'}$, aromatic), 7.30 (m, 2H, H^3, H,^{6} aromatic), 7.15 (m, 2H, H$^{4'}$, H$^{5'}$, aromatic), 6.85 (m, 2H, H,^{4} H,^{5} aromatic), 6.50 (d, J = 3.1 Hz, 1H, H$^{1'}$), 5.95 (dd, J_1 = 3.3 Hz, J_2 < 0.4 Hz, 1H, H$^{2'}$), 4.95 (dd, J_1 = 3.1 Hz, J_2 < 0.4 Hz, 1H, H^2), 4.75 (m, 2H, OCH$^{n'}$H$^{m'}$, OCH^{n}H^m), 4.50 (d, J = 3.2 Hz, 1H, H^1), 4.25 (m, 2H, OCH$^{n'}$H$^{m'}$, OCH^{n}H^m), 3.20 (dt, J_1 = 14.7, J_2 = 5.2, 1H, OCH$^{b'}$H$^{a'}$), 2.95 (m, 1H, CH$^{b'}$H$^{a'}$), 2.85 (dt, J_1 = 14.4, J_2 = 4.7, 1H, CH^{b}H^a), 2.70 (m, 1H, CH^{b}H^a), 0.15 (s, 9H, NSi(CH$_3$)$_3$), −0.20 (s, 9H, NSi(CH$_3$)$_3$). FT-Raman (cm^{-1}): 3122(m), 3085(m), 3044(m), 2976(m), 2961(m), 2902(s), 1608(w), 1529(m), 1482(m), 1470(sh), 1443(m), 1395(sh), 1380(m), 1337(s), 1285(m), 1267(m), 1230(w), 1180(m), 1154(w), 1129(w), 1003(m), 874(w), 798(m), 736(m), 668(w), 620(m), 587(w), 529(w), 442(w), 385(w), 292(m), 230(m), 147(m), 104(m).

The variable-temperature ^{1}H NMR spectra were recorded in [^{2}H$_8$]toluene and [^{2}H$_8$]tetrahydrofuran at −50, −25, 0, 30, and 50 °C. Still only one set of resonances of protons of the complex were observed, indicating the presence of solely *rac*-isomers in solution, and no isomerization occurs in the range of the above-mentioned temperatures (for more details see Supporting Information).

Synthesis of *rac*-[O(CH$_2$CH$_2$C$_9$H$_6$)$_2$]DyCH$_2$SiMe$_3$ (7). To a suspension of 1.43 g (2.51 mmol) of [O(CH$_2$CH$_2$C$_9$H$_6$)$_2$]DyCl-(THF) in 40 mL of toluene was added 0.23 g (2.55 mmol) of LiCH$_2$SiMe$_3$ at about 0 °C. The resulting suspension was allowed to warm to ambient temperature and stirred overnight under argon. The precipitate was separated by centrifugation, and the clear solution was concentrated. The residue was extracted with toluene−hexane (1:15, v/v). The hexane extract was cooled to −30 °C, and 0.68 g (51%) of **7** was obtained as yellow crystals. Anal. Calcd for C$_{26}$H$_{31}$OSiDy: C, 56.78; H, 5.64. Found: C, 56.38; H, 5.59. FT-Raman (cm^{-1}): 3080(m), 3044(s), 2947(m), 2895(s), 1525(m), 1480(m), 1463(sh), 1439(m), 1393(w), 1335(s), 1229(w), 1153(w), 1126(w), 1084(w), 1065(w), 1032(w), 1000(m), 873(w), 742(s), 689(w), 673(w), 642(m), 602(m), 529(w), 444(w), 394(w), 230(m), 146(s), 115(m).

Synthesis of *rac*-[O(CH$_2$CH$_2$C$_9$H$_6$)$_2$]YbCH$_2$SiMe$_3$ (8). A procedure similar to that for complex **7** was adopted for [O(CH$_2$CH$_2$C$_9$H$_6$)$_2$]YbCl(THF) (1.42 g, 2,45 mmol) and LiCH$_2$-SiMe$_3$ (0.24 g, 2.55 mmol), which afford **8** as violet crystals (0.61 g, 45%). Anal. Calcd for C$_{26}$H$_{31}$OSiYb: C, 55.71; H, 5.54. Found: C, 55.53; H, 5.79.

X-ray Structure Determination. Single crystals of **1** and **5** suitable for X-ray single-crystal diffraction were obtained by recrystallization in THF and toluene, respectively. Owing to air- and moisture-sensitivity, the single crystals of **1** and **5** were sealed in thin-walled glass capillaries. In the case of **1**, some mother liquor was added. Data were collected on a Rigaku AFC7R diffractometer with graphite-monochromated Mo Kα radiation, λ = 0.71069 Å, using the ω−2θ technique at 20 °C. The data were corrected for Lorentz−polarization effects; an empirical absorption correction was applied using the program DIFABS for **1** or based on azimuthal scans of several reflections for **5**. The structures were solved by direct methods for **1** or the heavy-atom Patterson method for **5** and expanded using Fourier techniques. The nonhydrogen atoms were refined anisotropically by full-matrix least squares. Hydrogen atoms were included but not refined. Scattering factors were taken from ref 17. All calculations were performed using the TEXSAN crystallographic software package.[18]

Polymerization of MMA. All polymerization reactions were carried out under argon. MMA was added to the solution of the initiator with vigorous magnetic stirring at the desired

(17) Cromer, D. T.; Waber, J. T. *International Tables for X-Ray Crystallography*; Kynoch Press: Birmingham, 1974; Vol. 4, Table 2.2A.
(18) *TEXSAN*, Crystal Structure Analysis Package; Molecular Structure Corporation: Houston, TX, 1985 and 1992.

temperature. After a certain time, the polymerization was quenched with acidified methanol, and the polymer was precipitated. The resulting polymer was washed with methanol and dried in a vacuum at 50 °C.

The *rac*/*meso* interconversion of the enolate complex at the prevailing polymerization is demonstrated by a ^{1}H NMR experiment: addition of 0.5 equiv of ^{i}PrOH, representing the approximate steric bulk of MMA, to a solution of **9** in [$^2H_8$]-tetrahydrofuran in an NMR tube at room temperature. Besides *rac*-[O($CH_2CH_2C_9H_6$)$_2$]YCH_2SiMe_3 (δ 6.37, $H^{1'}$, 5.94, $H^{2'}$) and *rac*-[O($CH_2CH_2C_9H_6$)$_2$]YO^iPr (δ 6.39, $H^{1'}$, 5.97, $H^{2'}$), the *meso*-[O($CH_2CH_2C_9H_6$)$_2$]YO^iPr (δ 6.62, H^1, 6.15, H^2) was observed. The ratio of *meso*-[O($CH_2CH_2C_9H_6$)$_2$]YO^iPr to *rac*-[O($CH_2CH_2C_9H_6$)$_2$]YO^iPr is about 1:3.

Acknowledgment. We are grateful to the National Science Foundation of China and the State Key Project of Basic Research (Project 973) (No. G2000048007) for financial support. We also thank Prof. Zhaomin Hou of RIKEN, Japan, for gel permeation chromatographic analyses and Dr. Liming Jiang of Zhejiang University for DSC analyses.

Supporting Information Available: Tables of atomic coordination, thermal parameters, and interatomic distances and angles for complexes **1** and **5**, variable-temperature ^{1}H NMR spectra of complex **6**, a table of selected two-dimensional ^{1}H NMR data for complex **2**, and a number scheme for the ^{1}H NMR of complex **2** with important NOEs. This material is available free of charge via the Internet at http://pubs. acs.org.

OM001060G